Enhancement of the Physical, Mechanical, and Thermal Properties of Epoxy-based Bamboo Nanofiber Nanocomposites

Samsul Rizal,[a] Asniza Mustapha,[b] F. A. T Owolabi,[b,c] H. P. S Abdul Khalil,[b,]* Ying Ying Tye,[b] H. M. Fizree,[b] C. K. Abdullah,[b] U. Seeta Uthaya Kumar,[b] and M. T. Paridah [d]

Epoxy-based nanocomposites were prepared by incorporating 0.3%, 0.5%, 0.7%, 1%, and 2% cellulose nanofibers (CNF) through a hand lay-up technique. The influence of the CNF as a reinforcement material on the morphology, and the physical, mechanical, and thermal properties of epoxy-based nanocomposites were investigated using scanning electron microscopy (SEM), density, void content, water absorption, tensile, flexural, impact strength, and thermogravimetric analyses. Compatibility between the nano-reinforcement and epoxy matrix was confirmed using SEM, which demonstrated that the CNF was homogeneously dispersed throughout the epoxy matrix. The mechanical properties were enhanced by increasing the CNF loading up to 1%. Moreover, the incorporation of CNF into the composites reduced the water uptake of the substrates in the water absorption test and resulted in a high thermal stability when exposed to a high temperature. Bamboo-CNF could be used as a potential reinforcement material to improve the properties of epoxy-based nanocomposites.

Keywords: Bamboo fiber; High pressure; High-pressure subcritical; Enzymatic hydrolysis; Morphological characterization; Thermal properties

*Contact information: a: Department of Mechanical Engineering, Syiah Kuala University, Banda Aceh 23111, Indonesia; b: School of Industrial Technology, Universiti Sains Malaysia, 11800 Penang, Malaysia; c: Federal Institute of Industrial Research Oshodi, Lagos, Nigeria; d: Institute of Tropical Forestry and Forest Products (INTROP), Universiti Putra Malaysia, 43400 Serdang, Selangor, Malaysia; *Corresponding author: akhalilhps@gmail.com*

INTRODUCTION

A cellulose nanofiber (CNF)-reinforced nanocomposite is a nanocomposite that contains a polymer matrix and nanoscale cellulose (1 nm to 100 nm) as a reinforcement material (Siqueira *et al.* 2010). Incorporation of nanocellulose as a reinforcement material in polymers is one approach that is used to develop new, high-end nanocomposites for various applications, such as in the automotive, construction, electronics, food packaging, and aerospace sectors (Sun and Yao 2011). Over the decades, traditional composites have been prepared using synthetic materials such as glass, carbon, or aramid fibers as fillers to reinforce epoxy, unsaturated polyester resins, polyurethanes, or phenolics. However, despite their good physical and mechanical properties enhancement in composite formulations, these materials have been experiencing various types of legislative restrictions and environmentalists' demands due to issues such as their non-biodegradability (Owolabi *et al.* 2017). The increasing interest in using cellulosic fibers as a filler or reinforcement material instead of synthetic fibers is a result of the biodegradability, renewability, sustainability, low weight, and low cost of cellulosic fibers, as well as their promising mechanical properties (Li *et al.* 2007; Dufresne 2010).

In addition to a better recyclability, higher flexibility, transparency, and lighter weight, nanocellulose-reinforced polymer nanocomposites are superior to conventional micro- and macro-composites in terms of their thermal, mechanical, and barrier properties, even at low reinforcement levels (Oksman *et al.* 2006; Sorrentino *et al*. 2007). Composites with nanoscale cellulose reinforcements exhibit a larger surface area and lower defects in the reinforcing components. This phenomenon results from the smaller diameter of the CNF and high surface area, which provides a greater interface for the polymers (Kamel 2007).

Cellulose nanofibers have been used extensively in the production of nanocomposites with a variety of thermoplastic and thermoset polymers, such as phenolic resin (Nakagaito and Yano 2005), epoxy resin (Masoodi *et al.* 2012), polyurethane (Seydibeyoğlu and Oksman 2008), styrene butyl acrylate (Malainine *et al.* 2005), and melamine formaldehyde (Henriksson and Berglund 2007). Epoxy resins are known to be one of the most versatile classes of polymers because of their excellent mechanical and electrical properties, good thermal stability, high stiffness, easy processing abilities, good resistance to chemicals, and absence of volatile compounds (Azeez *et al.* 2013; Mohan 2013). They are widely used in the fields of high-performance protective coatings, automotive primers, semiconductor encapsulates, dielectric materials, structural components, and composites (Pham and Marks 2002; Mohan 2013). However, cured epoxy resins possess some limitations, as its delamination, inherent brittleness, low impact resistance, and low fracture toughness behavior make it inadequate for certain end-use applications (Abdellaoui *et al.* 2015). Thus, more research is needed to enhance its physical and mechanical properties through the addition of additives, fillers, or reinforcement materials (Masoodi *et al.* 2012).

The properties of CNF-reinforced nanocomposites are influenced by the nature of the polymer matrix, CNF loading, particle size, aspect ratio, CNF-matrix adhesion, and CNF-CNF attraction (Ramazanov *et al.* 2010). Researchers have shown that different CNF loadings influence both the physical and mechanical properties of nanocomposites, such as by increasing the tensile strength and modulus of elasticity. It has also been reported that the addition of CNF restricts plastic deformation and is good for stress transfer (Gong *et al.* 2011; Bulota *et al.* 2012). Nanocomposites suffer from weak mechanical and thermal properties when the agglomeration of fiber occurs with the introduction of a high CNF loading percentage, which prevents the formation of a homogenous mixture. Saba *et al.* (2016) reported that the presence of agglomerates led to a reduction in the effective interaction volume, as well as large, continuous interfacial zones when 5% nanofiller was added to an epoxy matrix. In the studies by Shih (2007) and Abdul Khalil *et al.* (2013), it was reported that the incorporation of cellulose bamboo fiber improved the fracture toughness and impact properties of the polymer composite matrix. However, no remarkable enhancement in the flexural strength was observed, which was attributed to the poor compatibility between the cellulose fiber and polymer matrix. It is believed that poor matrix accessibility increases the interfacial tension between the cellulose fiber and polymer matrix, which increases the porosity of the composites (Reddy *et al.* 2013; Jawaid *et al.* 2014).

The increasing global interest in the exploration and development of nanocomposites has driven this study to develop environmentally friendly and sustainable nano-based materials that could provide an alternate way to employ locally available biomass for various advanced engineering applications. In a previous study, CNF from *Gigantochloa scortechinii* bamboo was successfully isolated and characterized using a chemo-mechanical technique.

Cellulose nanofiber-reinforced epoxy-based nanocomposites have been developed previously and improved some of the mechanical properties of neat epoxy composites (Saurabh *et al.* 2016). The present study was conducted to further examine the effect of a low CNF loading (0.3%, 0.5%, 0.7%, 1%, and 2%) on other properties of nanocomposites, including the physical, mechanical, and thermal stability properties.

EXPERIMENTAL

Materials

Gigantochloa scortechinii bamboo CNF was used as a reinforcement material and isolated in the manner described by Saurabh *et al.* (2016). The epoxy resin (D.E.R 331) and curing agent (Polyamine hardener 8161) were supplied by ZARM Scientific and Supplies Sdn. Bhd. (Penang, Malaysia) and used without any further processing.

Fabrication of the CNF-reinforced Epoxy Nanocomposites

The CNF isolated from *G. scortechinii* was freeze-dried (Freezone 2.5, Labconco, Kansas City, MO, USA) for 12 h and kept in a desiccator prior to fabrication of the composites. The epoxy resin and hardener were prepared at a ratio of 2:1 (w/w). Dried CNF was added at loading percentages of 0.3%, 0.5%, 0.7%, 1%, and 2% (w/w) to the epoxy resin and stirred using a high-speed mechanical stirrer for 30 min at room temperature. The hardener was added into the mixture and mechanically stirred for 10 min. The mixture was degassed in a vacuum chamber for 15 min. The mixture was then cast into a stainless-steel mold covered with a silicone spray releasing agent to facilitate removal of the cured composites. The mixture was left to cure at 85 °C for 2 h, and then post-curing occurred at 125 °C for 3 h.

Characterization

Morphological and compatibility analyses

The morphology and compatibility of the neat epoxy composite and CNF-reinforced epoxy-based nanocomposites were evaluated using scanning electron microscopy (SEM). The fractured surfaces of the composites were observed using SEM (EVO MA10, Carl Zeiss SMT, Oberkochen, Germany) with an accelerating voltage of 15 kV. Samples from the impact tests with a thickness of 2 mm were sputter-coated with a thin layer of gold prior to observation to prevent surface charging during analysis.

Density

The densities of the neat epoxy composite and CNF-reinforced epoxy-based nanocomposites were determined using an X-ray density profiler (Grecon Da-X, Alfeld, Germany), according to ASTM D1895 (2017). Samples were cut to the dimensions 50 mm × 50 mm × 4 mm. The samples were then inserted into their respective slots in the density profiler. The density profile of each sample was measured and recorded as the experimental density.

Void content

The theoretical and experimental densities of the nanocomposites were used to determine their void content. Determination of the void content was done using ASTM D2734 (2016). The void content percentage was calculated using Eq. 1, while the theoretical density was calculated using Eq. 2,

$$Void\ content\ (\%) = \frac{\rho_{theoretical} - \rho_{experimental}}{\rho_{theoretical}} \tag{1}$$

$$\rho_{theoretical} = \frac{1}{(\frac{W_f}{\rho_f} + \frac{W_m}{\rho_m})} \tag{2}$$

where $\rho_{theoretical}$ and $\rho_{experimental}$ are the theoretical and experimental densities (g/cm^3), respectively, W_f is the weight fraction of the filler (wt%), W_m is the weight fraction of the matrix (wt%), ρ_f is the density of the filler (g/cm^3), and ρ_m is the density of the matrix (g/cm^3).

Water absorption

The water absorption percentage of the composites was measured according to ASTM D570 (2010). The dimensions and weight of the composite samples were recorded prior to immersion in distilled water at room temperature. The weight and dimensions were recorded after 1 d, 3 d, 5 d, 7 d, 9 d, and 10 d, until a constant weight was reached.

All of the measurements were made at room temperature using a jaw-type Mitutoyo digital vernier caliper (Kawasaki, Japan), which has an accuracy of 0.01 mm. The water absorption percentage was calculated with Eq. 3,

$$Water\ absorption\ (\%) = \left(\frac{W_n - W_d}{W_d}\right) \times 100 \tag{3}$$

where W_d is the initial weight of the composite (g) and W_n is the final weight of the composite (g).

Tensile test

The neat epoxy composite and CNF-reinforced epoxy-based nanocomposites were cut to the dimensions 120 mm × 15 mm × 4 mm. The tensile modulus and tensile strength were determined according to ASTM D3039 (2017) using an Instron universal testing machine (UTM 5582, Ohio, USA). The testing speed and gauge length were 5 mm/min and 60 mm, respectively.

Flexural test

The flexural test was conducted according to ASTM D790 (2017). All of the samples were cut to the dimensions 160 mm × 20 mm × 4 mm. The three-point bending test was performed using an Instron Universal Testing Machine (UTM 5582) with a crosshead speed of 2 mm/min.

Impact test

The impact test was performed according to ASTM D256 (2010). Samples with the dimensions 70 mm × 15 mm × 4 mm were subjected to impact testing using an impact tester machine (Gotech GT-A1-7000L, Taichung City, Taiwan).

Thermal analysis

The degradation temperature and thermal stability analyses of the neat epoxy composite and CNF-reinforced epoxy-based nanocomposites were performed using thermogravimetric analysis (TGA) (TGA/SDTA 851; Mettler Toledo, Zurich, Switzerland).

All of the samples were heated from 30 °C to 800 °C under a nitrogen atmosphere at a heating rate of 20 °C/min.

RESULTS AND DISCUSSION

Physical Properties

Density

The density of a nanocomposite depends on the relative proportion of its constituents, matrix, and reinforcing materials. Experimental and theoretical densities of the neat epoxy composite and CNF-reinforced epoxy-based nanocomposites at various CNF loadings are displayed in Table 1. The average experimental and theoretical densities of the neat epoxy composite were 1.12 g/cm^3 and 1.14 g/cm^3, respectively. Both the experimental and theoretical densities of all of the nanocomposites increased with an increasing CNF loading. This result could have been because of the incorporation of high-density CNF (1.5 g/cm^3) with low-density epoxy resin (1.14 g/cm^3), which caused an increase in the density of the nanocomposites (Shimazaki *et al.* 2007; Lavoine *et al.* 2012). Density correlates to many composite performance characteristics, such as the mat/fiber structure, pressing environment, furnish characteristics (*i.e.*, compressibility, moisture content, and distribution), and hot-pressing conditions (*i.e.*, type, closing speed, temperature, pressure, duration, and step-closing schedules) (Suchsland and Woodson 1986; Wang and Winistorfer 2000; Wang *et al.* 2001).

Table 1. Density and Void Content of the CNF-reinforced Epoxy-based Nanocomposites at Various Bamboo-CNF Loadings

CNF Loading (wt.%)	Theoretical Density (g/cm^3)	Experimental Density (g/cm^3)	Void Content (%)
0	1.1400	1.1212	1.65
0.3	1.1408	1.1274	1.17
0.5	1.1414	1.1324	0.79
0.7	1.1419	1.1366	0.46
1.0	1.1427	1.1411	0.14
2.0	1.1455	1.1446	0.08

Void content

Voids are formed during composite processing. They result from the evaporation of volatile compounds and residual solvents during composite curing and entrapment of the resulting air bubbles (Abdul Khalil *et al.* 2013). The differences in the experimental and theoretical densities of the nanocomposites were ascribed to the presence of voids (Table 1). The void content of the nanocomposites decreased when the CNF loading increased from 0% to 2%. This development is attributed to a low absolute value of zeta potential of CNF, which tends to agglomerate when introduced to polymer matrix but that doesn’t mean that it will not blend with the polymer, depending on the level of agitation and as the quantity of the CNF increases. However, as more CNF is added to the matrix, the matrix voids get filled over the course of time, depending on the quantity of CNF added. From the study, addition of 2% CNF loading will go a long way in adequately achieving good (CNF) filler spread and very low void formation in the polymer composite. The decrease in the void content occurred because the voids were filled with CNF, which led to an enhancement of the mechanical properties of the nanocomposites. Moreover, the fatigue and strength properties of the nanocomposites were highly dependent upon the void content, as voids can promote and initiate failure by negatively impacting the stress transfer between the CNF and matrix (Svagan *et al.* 2007; Abdul Khalil *et al.* 2013). A low CNF loading also prevented agglomeration from occurring. Agglomeration can increase the void content of the final products because it prevents CNF from homogeneously filling voids.

Water absorption

The water absorption behavior of polymer-reinforced composites is dependent upon several factors, including the characteristics of the matrix-filler, processing techniques, immersion in water, and the constituents of the composites (Abdul Khalil *et al.* 2013). The water absorption behavior of the CNF-reinforced epoxy-based nanocomposites with various CNF loadings is illustrated in Fig. 1.

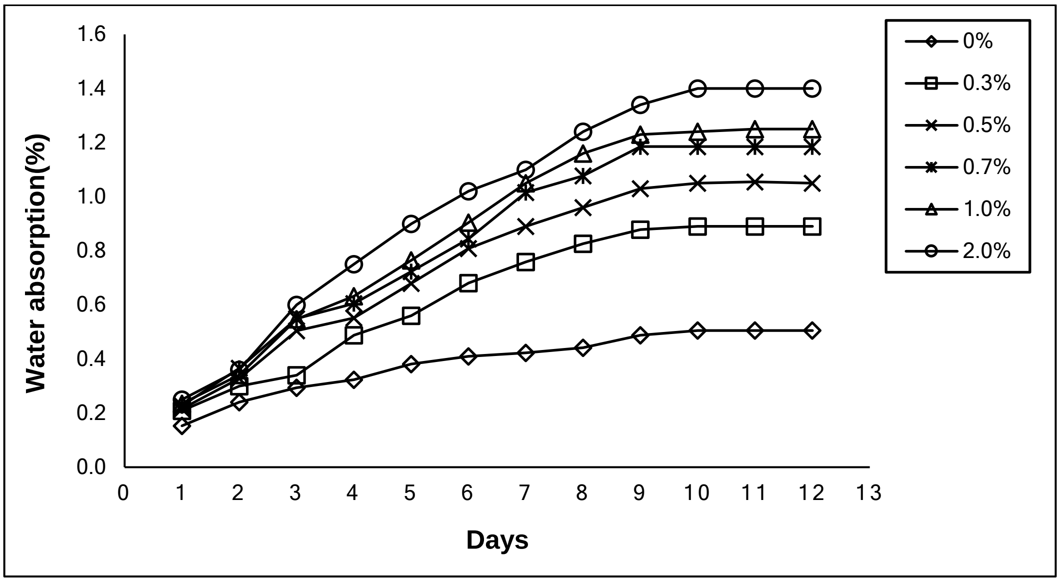

Fig. 1. Water absorption of the CNF-reinforced epoxy-based nanocomposites at various CNF loadings

A similar trend was observed for the water absorption percentage, with the percentage increasing for all of the samples as the CNF loading increased from 0% to 2%. This phenomenon indicated that the water capacity of the nanocomposites was influenced by the CNF loading. The hydrophilic nature of the CNF resulted in the nanocomposites being able to take up water and form hydrogen bonds (Lani *et al.* 2014). However, the value remained constant after 10 d of immersion in water, at which point the nanocomposites were saturated. The water absorption capacity of the nanocomposites was higher than that of the neat epoxy composite (Fig. 1). This occurrence was attributed to the hydrophobic nature of the epoxy resin, which has a low ability to absorb water compared with the CNF. The 2% CNF loading exhibited the highest water absorption percentage at 1.42%. This result was because of the higher amount of CNF present in the nanocomposites, and its hydrophilic nature resulted in more water uptake. Additionally, increasing the CNF loading increased the formation of hydrogen bonds between the CNF and water molecules.

The presence of voids and porosity in the nanocomposites also influenced the water intake of the nanocomposites, as was discussed earlier. The weight of the nanocomposites increased as water was trapped inside the voids. Thus, nanocomposites with a high void content increased the water absorption percentage, as they could absorb a higher amount of water. Water uptake by the neat epoxy composite only involved absorption of water into the voids of the composites, whereas water uptake by the CNF-reinforced epoxy-based nanocomposites involved the absorption of water into the voids and by the CNF. Therefore, the nanocomposite with a 2% CNF loading, which had the lowest void content, demonstrated the highest water uptake value (Table 1).

Mechanical Properties

The mechanical properties of the neat epoxy composite and CNF-reinforced epoxy-based nanocomposites were evaluated using tensile, flexural, and impact tests to investigate the influence of the CNF loading as a reinforcement material in the epoxy polymer. The overall mechanical properties are summarized in Table 2.

Table 2. Mechanical Properties of the CNF-reinforced Epoxy-based Nanocomposites with Various CNF Loadings

CNF Loading (% w/w)	Tensile			Flexural		Impact Strength (KJ/m²)
	Strength (MPa)	Modulus (GPa)	Elongation at break (%)	Strength (MPa)	Modulus (GPa)	
0	39.24±1.25	0.87±0.01	9.37±0.12	51.47±0.85	1.53±0.02	4.04±0.23
0.3	42.19±1.31	0.96±0.03	8.05±0.22	53.23±1.51	1.62±0.03	4.49±0.22
0.5	47.90±1.32	1.25±0.02	7.37±0.21	56.40±0.76	1.76±0.06	5.49±0.27
0.7	49.41±0.85	1.33±0.02	5.74±0.36	57.73±1.63	1.87±0.03	7.28±0.09
1.0	51.37±1.37	1.53±0.04	4.53±0.33	60.87±1.36	1.95±0.03	7.89±0.28
2.0	48.92±1.26	1.29±0.03	4.48±0.21	58.16±1.25	1.82±0.02	6.62±0.17

Value in parentheses = Standard deviation

From the result, the mechanical properties which include Tensile strength and Young’s modulus of the neat epoxy are 39.2 MPa and 0.87 GPa, respectively. The values are higher than the values reportedly obtained of similar epoxy resin of 24.6 MPa/ 0.291 GPa (Deng *et al.* 2013) and 7 MPa/115 GPa (Abdullah and Ansari 2015) for Tensile strength/Young’s Modulus respectively.

Tensile properties

The tensile strength of the nanocomposites increased as the CNF loading increased from 0% to 1%, but loadings higher than 1% caused a reduction in the tensile strength, with values in the range of 39 MPa to 51 MPa (Table 2). These results also showed that the nanocomposites were stiffer and tougher than the neat epoxy composite, as they exhibited higher tensile strengths. The 1% CNF-reinforced nanocomposite demonstrated the highest tensile strength at 51.4 MPa, while the neat epoxy composite showed the lowest tensile strength at 39.2 MPa. This result was attributed to the relatively homogenous dispersion of the low CNF content in the epoxy matrix. Moreover, the small size and high surface area of the CNF could have provided more interface area, which led to good interfacial bonding between the CNF and epoxy matrix (Svagan *et al.* 2007). This bonding prevented quick crack propagation and promoted better stress transfer between these two components. This interaction consequently led to an enhanced tensile strength in the reinforced nanocomposites (Lani *et al.* 2014). However, the maximum tensile strength was observed at the 1% CNF loading (Table 2). This result likely occurred because agglomeration tended to occur when the highest concentration (2%) of CNF was introduced into the matrix. The hydrophilic nature of the cellulosic fibers and the aggregated areas would act as stress concentration points that led to failure or early rupture and caused a reduction in the tensile strength (Saba *et al.* 2016). This phenomenon could be further verified using SEM.

The tensile modulus was observed to have a similar trend as that of the tensile strength, where it also increased as the CNF loading increased from 0% to 1%. The CNF-reinforced epoxy-based nanocomposites clearly showed higher tensile modulus values compared with that of the neat epoxy composite, with the 1% CNF loading exhibiting the highest tensile modulus of 1.53 GPa. This result also demonstrated that CNF has the ability to stiffen the epoxy matrix, as the incorporation of CNF increased the tensile modulus of the nanocomposites. This result was accredited to good adhesion between CNF and the epoxy polymer matrix, as shown through the SEM images. This led to favourable interaction between the CNF and matrix, and the homogeneity of the nanocomposites. Such results also can be attributed to the nanoscale of the fibrils. The good dispersion of small-diameter CNF in the epoxy matrix led to eventual closure of the space (void) in the polymer fibril-matrix through the filling of the voids by the CNF particles, hence reducing the void contents in the composites (Svagan *et al.* 2007). The decrease in the free space between the particles, which is also known as the inter-particle distance, led to a reduction in the flexibility of the polymer chain, and therefore, increased the tensile modulus (Abdul Khalil *et al.* 2013). However, the presence of agglomerates in the 2% CNF-reinforced epoxy-based nanocomposites decreased the tensile modulus.

In contrast to both the tensile strength and modulus, the elongation at break of the nanocomposites decreased with an increasing CNF loading (Table 2). The neat epoxy composite exhibited the highest elongation at break of 9.37%, whereas the nanocomposite with a 2% CNF loading demonstrated the lowest value of 4.48%. This reduction in the elongation at break was attributed to fiber aggregation, which formed stress concentration points that require less energy to propagate cracks when a load is applied. Hence, the stress was unable to efficiently transfer near the flaws during tensile deformation and resulted in failure (Pan *et al.* 2009). This result was also explained by the greater rigidity of the CNF compared with the brittle nature of the epoxy, which diminished the amount of existing epoxy for elongation (Abdul Khalil *et al.* 2013). Moreover, the reduction in the elongation at break upon incorporation of CNF occurred because of the decline in deformability of the interface between the epoxy matrix and CNF (Husseinsyah and Mostapha 2011). An excess amount of CNF also led to an increase in the intermolecular interaction that might compete and interfere with the interactions between the CNF and epoxy resin. This occurrence caused the miscibility and compatibility of the nanocomposite system to be reduced, and therefore, decreased the elongation at break of the nanocomposites (Svagan *et al.* 2007; Lani *et al.* 2014).

Flexural properties

Increasing the CNF loading from 0.3% to 1% boosted both the flexural strength and modulus of the nanocomposites. This result demonstrated that the addition of small quantities of CNF to the epoxy matrix is effective as a reinforcement material in nanocomposites. The flexural strength of the neat epoxy composite gradually increased from 51.5 MPa to 60.9 MPa in the 1% CNF nanocomposite (Table 2). Meanwhile, the flexural modulus also increased from 1.53 GPa in the neat epoxy composite to 1.95 GPa in the 1% CNF nanocomposite. This increase in the flexural strength was attributed to the small size of the CNF, which provided more surface area, as well as the good interaction and bonding between the CNF and epoxy matrix, which resulted in a better stress transfer; therefore, the elastic deformation of the nanocomposites increased. Additionally, the quality of the interface in the composites is determined by the static adhesion strength and interfacial stiffness. These factors play a crucial role in the stress transfer ability of the material from the epoxy matrix to the CNF, as well as the elastic deformation. Therefore, the gradual increase in the stiffness and flexural strength of the nanocomposites indicated that stress was effectively transferred *via* the interface. In short, the interfacial adhesion of the CNF-epoxy matrix, coupled with the good dispersion of CNF in the matrix, restricted the mobility of the matrix chain upon loading and improved the flexural properties (Wu *et al.* 2010; Abdul Khalil *et al.* 2013). In the case of the 2% CNF loading, the nanocomposite exhibited a lower flexural strength than that of the 1% CNF-reinforced epoxy-based nanocomposite. As was stated earlier, the existence of agglomerates might have prevented strong interactions between the CNF and epoxy matrix and reduced the homogeneity of the nanocomposites. Clumping of the CNF acted as the weak point when stress was applied, which resulted in failure. This phenomenon could be further verified using SEM.

Impact strength

The impact strength of a composite is defined as the ability of the polymer to absorb energy during crack propagation and quick impact loading in the matrix (Seydibeyoğlu *et al.* 2013). According to Table 2, the impact strength of the nanocomposites increased with the addition of CNF compared with the neat epoxy composite. The maximum impact strength (7.89 kJ/m^2) was observed at the 1% CNF loading. However, increasing the CNF loading up to 2% caused a reduction in the impact strength. Increasing the CNF loading led to an incremental change in the impact strength as a result of the small size of the CNF, which provided a higher surface area (Seydibeyoğlu *et al.* 2013). Rapid crack propagation is initiated when a composite is subjected to an impact. When the crack propagation reaches the CNF in the composite, the CNF absorbs the impact energy and stops the crack propagation if there are strong interfacial interactions between the CNF and epoxy matrix (Abdul Khalil *et al.* 2013). In contrast, it was believed that the presence of CNF agglomerates favored poor interfacial adhesion in the 2% CNF loading and thus, restricted the ability of the nanocomposite to act against crack propagation as effectively as the rest of the nanocomposites. It then consequently propagated a catastrophic crack and lowered the impact strength (Steele *et al.* 2012). It was concluded from the results of this study that the incorporation of CNF as a reinforcement material, even at low loadings, enhanced the impact properties of the nanocomposites.

Morphological and Compatibility Analyses

Fracture surface morphology

The SEM micrographs of the cross-sections of the impact-fractured surfaces of the neat epoxy composite and CNF-reinforced epoxy-based nanocomposites are illustrated in Fig. 2. Variations in the surface morphology of the composites, including crack propagation, interface bonding, and dispersion of the CNF in the polymer matrix, were observed. Figure 2a shows that the surface of the neat epoxy composite was smooth and had a glassy exterior, which was indicative of its typical brittle nature. The pattern of cracks indicated that the brittleness of the pure epoxy composite resulted in a low resistance against crack propagation during tensile or impact fracturing and thus, lowered the mechanical strength (Dadfar and Ghadami 2013; Quan and Ivankovic 2015). The cracks seen in the image were believed to propagate from the bottom to the top of the composite. Figures 2b to 2f show the SEM micrographs of the fractured surfaces of the 0.3%, 0.5%, 0.7%, 1%, and 2% CNF-reinforced nanocomposites. These micrographs reveal that the pattern of cracks for all of the nanocomposites were relatively different than that of the neat epoxy composite. The images of the CNF-reinforced nanocomposites exhibit rough fractured surfaces with the presence of white dots, which are the CNF. Moreover, the roughness and irregular fractured surface of the nanocomposites showed that they were relatively less brittle, with the presence of sharp edges and deep line markings between the surfaces of the cracks, which resulted from rapid crack propagation (Yang *et al.* 2011; Saurabh *et al.* 2016).

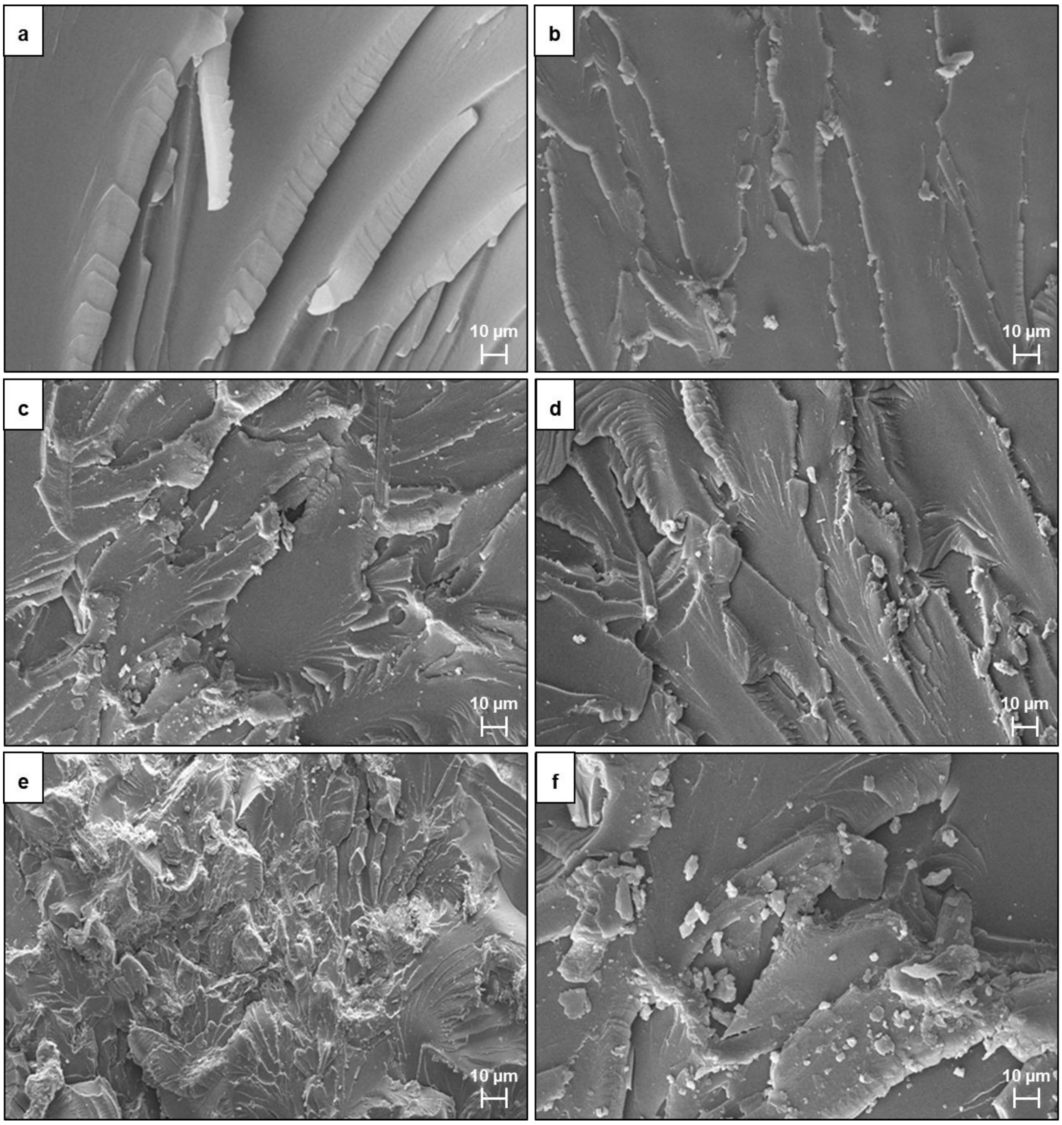

Fig. 2. SEM micrographs of the fractured surfaces of the (a) neat epoxy, and (b) 0.3%, (c) 0.5%, (d) 0.7%, (e) 1%, and (f) 2% CNF-reinforced epoxy-based nanocomposites

The fractured surfaces of the nanocomposites with 0.5% and 0.7% CNF loadings did not show remarkable differences (Figs. 2c and 2d). This result could have been attributed to the good dispersion and distribution of the CNF without aggregation in the nanocomposites, as the reinforcement was introduced at a low loading percentage. Proper dispersion and strong adhesion between the CNF and epoxy matrix resulted in an improved tensile strength and modulus in the nanocomposites. Similar to the neat epoxy composite, cracks in the CNF-reinforced epoxy-based nanocomposites were believed to have propagated from the bottom to the top. Noticeably, a deep line marking with no particle clumping was observed, and the surface became rougher and more jagged with CNF loadings higher than 1%. This change was because of the higher amounts of energy needed to break the nanocomposites, as the well-dispersed CNF hindered the crack propagation pathway (Liu *et al.* 2011). Better resistance towards crack propagation resulted in an increase in the tensile and impact properties of the CNF-reinforced epoxy nanocomposites with CNF loadings up to 1%.

The 2% CNF nanocomposite suffered from a coarser texture with no wavy or deep line markings, which was in contrast with the other samples. The addition of 2% CNF to the neat epoxy caused the CNF to agglomerate in certain spaces and reduced the effective interaction volume between the CNF and matrix. In this case, increasing the CNF concentration in the matrix up to a certain level will cause agglomeration to occur, which is the result of poor dispersion and distribution of the CNF in the selected area of the nanocomposites. The presence of agglomerates promoted blank spaces within the matrix and caused poor CNF dispersion. Agglomeration leads to void formation, which in turn could result in debonding of the matrix from the filler particles; this is expected to lower the tensile strength as a result of weak interfacial bonding between the reinforcement material and polymer matrix (Owolabi *et al*. 2017). Instead of individual nanofibers, the agglomerated structure of the CNF would act as a stress concentration point instead of being a reinforcement point. This stress concentration would then cause the cracks to penetrate through the agglomerated structure and form a weak point, which would initiate failure in the impact test (Jonoobi *et al.* 2012). No large clumps of CNF were observed in the SEM micrographs when a low amount of CNF (up to 1% w/w) was added to the epoxy matrix. Addition of CNF beyond 1% could reduce the mechanical properties of the nanocomposites, as was discussed earlier.

Thermal Properties

Thermogravimetric analysis

The TGA and differential thermogravimetric (DTG) curves of the nanocomposites are illustrated in Figs. 3 and 4, respectively. The initial degradation temperature (T_{onset}), maximum degradation temperature (T_{max}), and char residue of each of the samples are displayed in Table 3.

Table 3. Thermal Properties of the CNF-reinforced Epoxy-based Nanocomposites with Various CNF Loading

CNF Loading (%)	Initial Degradation Temperature, T_{onset} (°C)	Maximum Degradation Temperature, T_{max} (°C)	Residue (%)
0	309.14	383.66	9.66
0.3	344.93	386.86	8.28
0.5	346.80	387.69	8.71
0.7	347.53	388.15	8.53
1.0	348.79	389.54	8.31
2.0	347.26	387.17	8.64

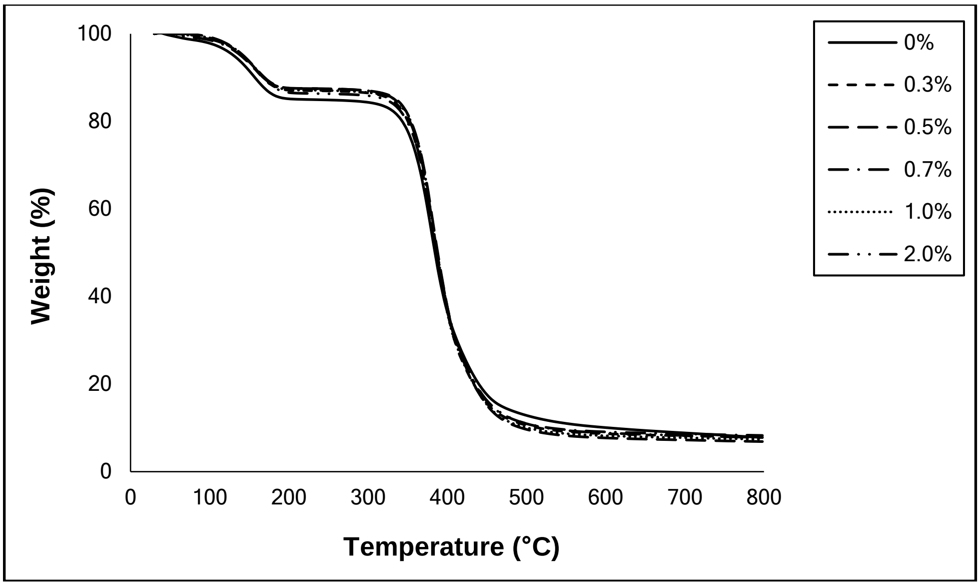

Fig. 3. TGA thermograms of the CNF-reinforced epoxy-based nanocomposites with various CNF loadings

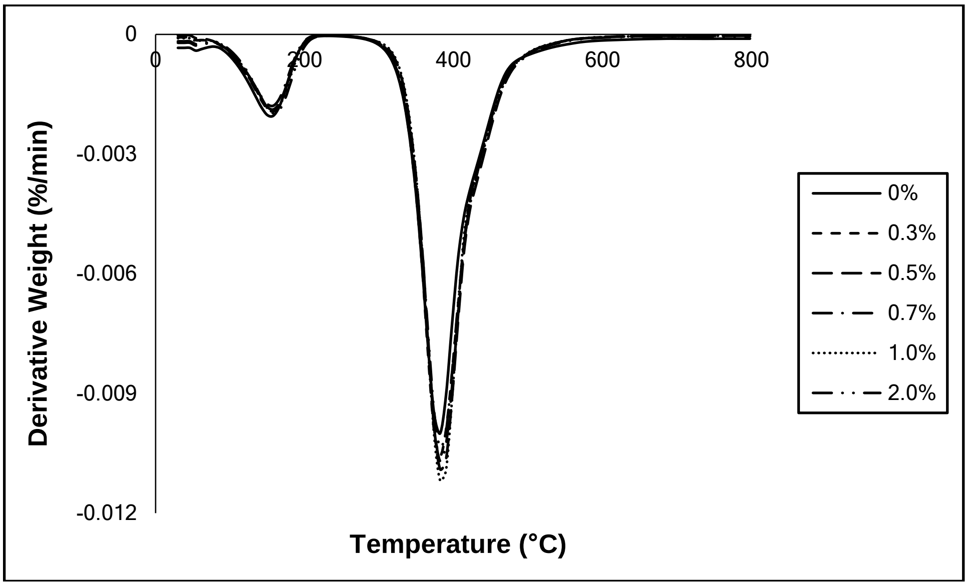

Fig. 4. DTG curves of the CNF-reinforced epoxy-based nanocomposites with various CNF loadings

All of the samples demonstrated initial weight losses below 100 °C, which was attributed to the evaporation of moisture. The T_{onset} of the neat epoxy composite was 309.1 °C, whereas the nanocomposites with 0.3%, 0.5%, 0.7%, 1%, and 2% CNF loadings exhibited T_{onset} values of 344.9 °C, 346.8 °C, 347.5 °C, 348.8 °C, and 347.3 °C, respectively. The T_{onset} values showed that the thermal stability of the nanocomposites slightly increased as the CNF loading increased from 0.3% to 1%. However, a slight decrease in the T_{onset} was observed for the 2% CNF loading. The DTG curves show that the neat epoxy composite exhibited a T_{max} of 383.7 °C. The T_{max} values of the 0.3%, 0.5%, 0.7%, 1%, and 2% CNF nanocomposites were observed to be 386.9 °C, 387.7 °C, 388.2 °C, 389.5 °C, and 387.2 °C, respectively. The T_{max} values of the nanocomposites were higher than that of the neat epoxy composite, and increased to 389.5 °C from 0.3% to 1% CNF loadings. Similar to the T_{onset}, the 2% CNF loading caused a reduction in the T_{max}. Furthermore, the amount of char residue at 800 °C gradually decreased with the addition of CNF from 0% to 2% and was in the range of 8.3% to 9.7%.

The addition of CNF at a low loading increased the thermal stability of the nanocomposites. This result was consistent with the high thermal degradation temperature of the CNF itself, coupled with the strong bonding between the CNF and epoxy matrix. This strong bonding resulted from the increased cross-linking of the epoxy resin and CNF, and the simultaneously reduced fiber-matrix interaction. The improvement in the thermal stability of the nanocomposites could also have been attributed to the high dispersion of the nanofibers in the epoxy matrix. The high thermal degradation temperature allowed the CNF to absorb and shield more heat in the matrix (He *et al.* 2011; Cross *et al.* 2013). There was also a limitation to the increase in the thermal stability with an increasing CNF loading. In this case, a CNF loading above 1% resulted in a slight reduction in the thermal stability. Agglomeration tended to occur as the CNF had a strong tendency to interact with itself to minimize its surface energy when a high concentration of CNF was introduced (Zare 2016). The agglomeration caused the CNF-CNF interaction to be stronger than the CNF-matrix interaction. The CNF did not impose any restriction on the molecular mobility, and therefore, decreased the thermal stability of the nanocomposite (Zhou *et al.* 2012).

CONCLUSIONS

1. Cellulose nanofibers displayed excellent reinforcing effects, which led to remarkable improvements in the overall properties of the epoxy-based nanocomposites.
2. The compatibility and surface morphology study using SEM indicated that the cellulose nanofibers (CNF) were homogeneously dispersed throughout the epoxy matrix when a low CNF loading was used.
3. The addition of up to 1% CNF resulted in a good distribution of nanofibers, with no evidence of agglomeration.
4. The strong interfacial bonding between the CNF and epoxy matrix resulted in improved tensile, flexural, and impact properties in the CNF-reinforced epoxy-based nanocomposites. The 2% CNF loading caused a decrease in the mechanical properties.
5. It was evident that agglomeration and poor dispersion of the CNF weakened the properties of the nanocomposite with a 2% CNF loading.
6. The TGA confirmed that the thermal stability of the nanocomposites was also improved with the addition of CNF.

ACKNOWLEDGEMENTS

The authors would like to thank the Ministry of Higher Education for the Fundamental Research Grant Scheme-Malaysia's Rising Star Award 2015 (FRGS-203/PTEKIND/6711531). The authors also would like to extend thanks to the research support and collaborations from the Mechanical Engineering Department, Syiah Kuala University, Indonesia, INTROP, UPM, Malaysia and the Federal Institute of Industrial Research Oshodi, Lagos Nigeria.

REFERENCES CITED

Abdellaoui, H., Bensalah, H., Echaabi, J., Bouhfid, R., and Qaiss, A. (2015). "Fabrication, characterization and modelling of laminated composites based on woven jute fibres reinforced epoxy resin," *Mater. Design* 68, 104-113. DOI: 10.1016/j.matdes.2014.11.059

Abdul Khalil, H. P. S., Fizree, H. M., Bhat, A., Jawaid, M., and Abdullah, C. K. (2013). "Development and characterization of epoxy nanocomposites based on nano-structured oil palm ash," *Compos. Part B-Eng.* 53, 324-333. DOI: 10.1016/j.compositesb.2013.04.013

Abdullah, S. I., and Ansari, M. N. M. (2015). "Mechanical properties of graphene oxide (GO)/epoxy composites," *Hbrc Journal* 11(2), 151-156.

ASTM D1895 (2017). "Standard test methods for apparent density, bulk factor, and pourability of plastic materials," ASTM International, West Conshohocken, PA.

ASTM D256 (2010). "Standard test methods for determining the Izod pendulum impact resistance of plastics," ASTM International, West Conshohocken, PA.

ASTM D2734 (2016). "Standard test methods for void content of reinforced plastics," ASTM International, West Conshohocken, PA.

ASTM D3039 (2017). “Standard test method for tensile properties of polymer matrix composite materials,” ASTM International, West Conshohocken, PA.

ASTM D570-98 (2010). “Standard test method for water absorption of plastics,” ASTM International, West Conshohocken, PA.

ASTM D790 (2017). “Standard test methods for flexural properties of unreinforced and reinforced plastics and electrical insulating materials,” ASTM International, West Conshohocken, PA.

Azeez, A. A., Rhee, K. Y., Park, S. J., and Hui, D. (2013). “Epoxy clay nanocomposites – Processing, properties and applications: A review,” *Compos. Part B-Eng.* 45(1), 308-320. DOI: 10.1016/j.compositesb.2012.04.012

Bulota, M., Kreitsmann, K., Hughes, M., and Paltakari, J. (2012). “Acetylated microfibrillated cellulose as a toughening agent in poly(lactic acid),” *J. Appl. Polym. Sci.* 126(S1), 448-457. DOI: 10.1002/app.36787

Cross, L., Schueneman, G., Mintz, E., Xu, S., Girouard, N., Shofner, M., and Meredith, C. (2013). “Nanocellulose reinforced epoxy elastomer,” in: *Proceedings of the 36th Annual Meeting of the Adhesion*, Daytona Beach, FL.

Dadfar, M. R., and Ghadami, F. (2013). “Effect of rubber modification on fracture toughness properties of glass reinforced hot cured epoxy composites,” *Mater. Design* 47, 16-20. DOI: 10.1016/j.matdes.2012.12.035

Deng, L., Ha, C., Sun, C., Zhou, B., Yu, J., Shen, M., and Mo, J. (2013). “Properties of bio-based epoxy resins from rosin with different flexible chains,” *Industrial & Engineering Chemistry Research* 52(37), 13233-13240.

Dufresne, A. (2010). “Processing of polymer nanocomposites reinforced with polysaccharide nanocrystals,” *Molecules* 15(6), 4111-4128. DOI: 10.3390/molecules15064111

Gong, G., Pyo, J., Mathew, A. P., and Oksman, K. (2011). “Tensile behavior, morphology and viscoelastic analysis of cellulose nanofiber reinforced (CNF) polyvinyl acetate (PVAc),” *Compos. Part A-Appl. S* 42(9), 1275-1282. DOI: 10.1016/j.compositesa.2011.05.009

He, H., Li, K., Wang, J., Sun, G., Li, Y., and Wang, J. (2011). “Study on thermal and mechanical properties of nano-calcium carbonate/epoxy composites,” *Mater. Design* 32(8-9), 4521-4527. DOI: 10.1016/j.matdes.2011.03.026

Henriksson, M., and Berglund, L. A. (2007). “Structure and properties of cellulose nanocomposite films containing melamine formaldehyde,” *J. Appl. Polym. Sci.* 106(4), 2817-2824. DOI: 10.1002/app.26946

Husseinsyah, S., and Mostapha, M. (2011). “The effect of filler content on properties of coconut shell filled polyester composites,” *Malaysian Polym. J.* 6(1), 87-97.

Jawaid, M., Alothman, O. Y., Paridah, M. T., and Abdul Khalil, H. P. S. (2014). “Effect of oil palm and jute fiber treatment on mechanical performance of epoxy hybrid composites,” *Int. J. Polym. Anal. Ch.* 19(1), 62-69. DOI: 10.1080/1023666X.2014.858429

Jonoobi, M., Mathew, A. P., Abdi, M. M., Makinejad, M. D., and Oksman, K. (2012). “A comparison of modified and unmodified cellulose nanofiber reinforced polylactic acid (PLA) prepared by twin screw extrusion,” *J. Polym. Environ.* 20(4), 991-997. DOI: 10.1007/s10924-012-0503-9

Kamel, S. (2007). “Nanotechnology and its applications in lignocellulosic composites, a mini review,” *Express Polym. Lett.* 1(9), 546-575. DOI: 10.3144/expresspolymlett.2007.78

Lani, N. S., Ngadi, N., Johari, A., and Jusoh, M. (2014). “Isolation, characterization, and application of nanocellulose from oil palm empty fruit bunch fiber as nanocomposites,” *J. Nanomater.* 2014. DOI: 10.1155/2014/702538

Lavoine, N., Desloges, I., Dufresne, A., and Bras, J. (2012). "Microfibrillated cellulose - Its barrier properties and applications in cellulosic materials: A review," *Carbohyd. Polym.* 90(2), 735-764. DOI: 10.1016/j.carbpol.2012.05.026

Li, X., Tabil, L. G., and Panigrahi, S. (2007). "Chemical treatments of natural fiber for use in natural fiber-reinforced composites: A review," *J. Polym. Environ.* 15(1), 25-33. DOI: 10.1007/s10924-006-0042-3

Liu, H.-Y., Wang, G.-T., Mai, Y.-W., and Zheng, Y. (2011). "On fracture toughness of nano-particle modified epoxy," *Compos. Part B-Eng.* 42(8), 2170-2175. DOI: 10.1016/j.compositesb.2011.05.014

Malainine, M. E., Mahrouz, M., and Dufresne, A. (2005). "Thermoplastic nanocomposites based on cellulose microfibrils from *Opuntia ficus-indica* parenchyma cell," *Compos. Sci. Technol.* 65(10), 1520-1526. DOI: 10.1016/j.compscitech.2005.01.003

Masoodi, R., El-Hajjar, R. F., Pillai, K. M., and Sabo, R. (2012). "Mechanical characterization of cellulose nanofiber and bio-based epoxy composite," *Mater. Design* 36, 570-576. DOI: 10.1016/j.matdes.2011.11.042

Mohan, P. (2013). "A critical review: The modification, properties, and applications of epoxy resins," *Polym.-Plast. Technol.* 52(2), 107-125. DOI: 10.1080/03602559.2012.727057

Nakagaito, A. N., and Yano, H. (2005). "Novel high-strength biocomposites based on microfibrillated cellulose having nano-order-unit web-like network structure," *Appl. Phys. A-Mater.* 80(1), 155-159. DOI: 10.1007/s00339-003-2225-2

Oksman, K., Mathew, A. P., Bondeson, D., and Kvien, I. (2006). "Manufacturing process of cellulose whiskers/polylactic acid nanocomposites," *Compos. Sci. Technol.* 66(15), 2776-2784. DOI: 10.1016/j.compscitech.2006.03.002

Owolabi, A. F., Saurabh, C. K., Dungani, R., & Khalil, H. A. (2017). "Spectroscopy and microscopy of microfibrillar and nanofibrillar composites". In Micro and Nano Fibrillar Composites (MFCs and NFCs) from Polymer Blends (pp. 279-299). https://doi.org/10.1016/B978-0-08-101991-7.00012-1.

Pan, P., Liang, Z., Cao, A., and Inoue, Y. (2009). "Layered metal phosphonate reinforced poly(L-lactide) composites with a highly-enhanced crystallization rate," *ACS Appl. Mater. Interf.* 1(2), 402-411. DOI: 10.1021/am800106f

Pham, H. Q., and Marks, M. J. (2002). "Epoxy resins," in: *Encyclopedia of Polymer Science and Technology*, H. F. Mark (ed.), John Wiley & Sons, Inc.

Quan, D., and Ivankovic, A. (2015). "Effect of core shell rubber (CSR) nano-particles on mechanical properties and fracture toughness of an epoxy polymer," *Polymer* 66, 16-28. DOI: 10.1016/j.polymer.2015.04.002

Ramazanov, M. A., Ali-Zade, R. A., and Agakishieva, P. B. (2010). "Structure and magnetic properties of nanocomposites on the basis PE + Fe_3O_4 и PVDF + Fe_3O_4," *Dig. J. Nanomater. Bios.* 5(3), 727-733.

Reddy, K. O., Maheswari, C. U., Shukla, M., Song, J. I., and Rajulu, A. V. (2013). "Tensile and structural characterization of alkali treated *Borassus* fruit fine fibers," *Compos. Part B-Eng.* 44(1), 433-438. DOI: 10.1016/j.compositesb.2012.04.075

Saba, N., Tahir, P. M., Abdan, K., and Ibrahim, N. A. (2016). "Fabrication of epoxy nanocomposites from oil palm nano filler: Mechanical and morphological properties," *BioResources* 11(3), 7721-7736. DOI: 10.15376/biores.11.3.7721-7736

Saurabh, C. K., Mustapha, A., Masri, M. M., Owolabi, A. F., Syakir, M. I., Dungani, R., Paridah, M. T., Jawaid, M., and Abdul Khalil, H. P. S. (2016). "Isolation and characterization of cellulose nanofibers from *Gigantochloa scortechinii* as a reinforcement material," *J. Nanomater.* 2016. DOI: 10.1155/2016/4024527

Seydibeyoğlu, M. O., and Oksman, K. (2008). "Novel nanocomposites based on polyurethane and micro fibrillated cellulose," *Compos. Sci. Technol.* 68(3-4), 908-914. DOI: 10.1016/j.compscitech.2007.08.008

Seydibeyoğlu, M. O., Misra, M., Mohanty, A., Blaker, J. J., Lee, K.-Y., Bismarck, A., and Kazemizadeh, M. (2013). "Green polyurethane nanocomposites from soy polyol and bacterial cellulose," *J. Mater. Sci.* 48(5), 2167-2175. DOI: 10.1007/s10853-012-6992-z

Shih, Y.-F. (2007). "Mechanical and thermal properties of waste water bamboo husk fiber reinforced epoxy composites," *Mat. Sci. Eng. A-Struct.* 445-446, 289-295. DOI: 10.1016/j.msea.2006.09.032

Shimazaki, Y., Miyazaki, Y., Takezawa, Y., Nogi, M., Abe, K., Ifuku, S., and Yano, H. (2007). "Excellent thermal conductivity of transparent cellulose nanofiber/epoxy resin nanocomposites," *Biomacromolecules* 8(9), 2976-2978. DOI: 10.1021/bm7004998

Siqueira, G., Bras, J., and Dufresne, A. (2010). "Cellulosic bionanocomposites: A review of preparation, properties and applications," *Polymers-Basel* 2(4), 728-765. DOI: 10.3390/polym2040728

Sorrentino, A., Gorrasi, G., and Vittoria, V. (2007). "Potential perspectives of bio-nanocomposites for food packaging applications," *Trends Food Sci. Tech.* 18(2), 84-95. DOI: 10.1016/j.tifs.2006.09.004

Steele, J., Dong, H., Snyder, J. F., Orlicki, J. A., Reiner, R. S., and Rudie, A. W. (2012). "Nanocellulose reinforcement of transparent composites," in: *Proceedings of SAMPE*, Baltimore, MD.

Suchsland, O., and Woodson, G. E. (1986). *Fiberboard Manufacturing Practices in the United States*, USDA Forest Service, Madison, WI.

Sun, D., and Yao, Y. (2011). "Synthesis of three novel phosphorus-containing flame retardants and their application in epoxy resin," *Polym. Degrad. Stabil.* 96(10), 1720-1724. DOI: 10.1016/j.polymdegradstab.2011.08.004

Svagan, A. J., Samir, M. A. S. A., and Berglund, L. A. (2007). "Biomimetic polysaccharide nanocomposites of high cellulose content and high toughness," *Biomacromolecules* 8(8), 2556-2563. DOI: 10.1021/bm0703160

Wang, S., and Winistorfer, P. M. (2000). "Fundamentals of vertical density profile formation in wood composites. Part 2. Methodology of vertical density formation under dynamic condition," *Wood Fiber Sci.* 32, 220-238.

Wang, S., Winistorfer, P. M., Young, T. M., and Helton, C. (2001). "Step-closing pressing of medium density fibreboard; Part 1. Influences on the vertical density profile," *Holz Roh. Werkst.* 59(1), 19-26. DOI: 10.1007/s001070050466

Wu, Y., Wang, S., Zhou, D., Xing, C., Zhang, Y., and Cai, Z. (2010). "Evaluation of elastic modulus and hardness of crop stalks cell walls by nano-indentation," *Bioresour. Technol.* 101(8), 2867-2871. DOI: 10.1016/j.biortech.2009.10.074

Yang, S.-Y., Lin, W.-N., Huang, Y.-L., Tien, H.-W., Wang, J.-Y., Ma, C.-C. M., Li, S.-M., and Wang, Y.-S. (2011). "Synergetic effects of graphene platelets and carbon nanotubes on the mechanical and thermal properties of epoxy composites," *Carbon* 49(3), 793-803. DOI: 10.1016/j.carbon.2010.10.014

Zare, Y. (2016). "Modeling the yield strength of polymer nanocomposites based upon nanoparticle agglomeration and polymer-filler interphase," *J. Colloid Interf. Sci.* 467, 165-169. DOI: 10.1016/j.jcis.2016.01.022

Zhou, Y. M., Fu, S. Y., Zheng, L. M., and Zhan, H. Y. (2012). "Effect of nanocellulose isolation techniques on the formation of reinforced poly(vinyl alcohol) nanocomposite films," *Express Polym. Lett.* 6(10), 794-804. DOI: 10.3144/expresspolymlett.2012.85

Article submitted: March 28, 2018; Peer review completed: July 7, 2018; Revised version received: July 15, 2018; Accepted: July 27, 2018; Published: August 27, 2018. DOI: 10.15376/biores.13.4.7709-7725